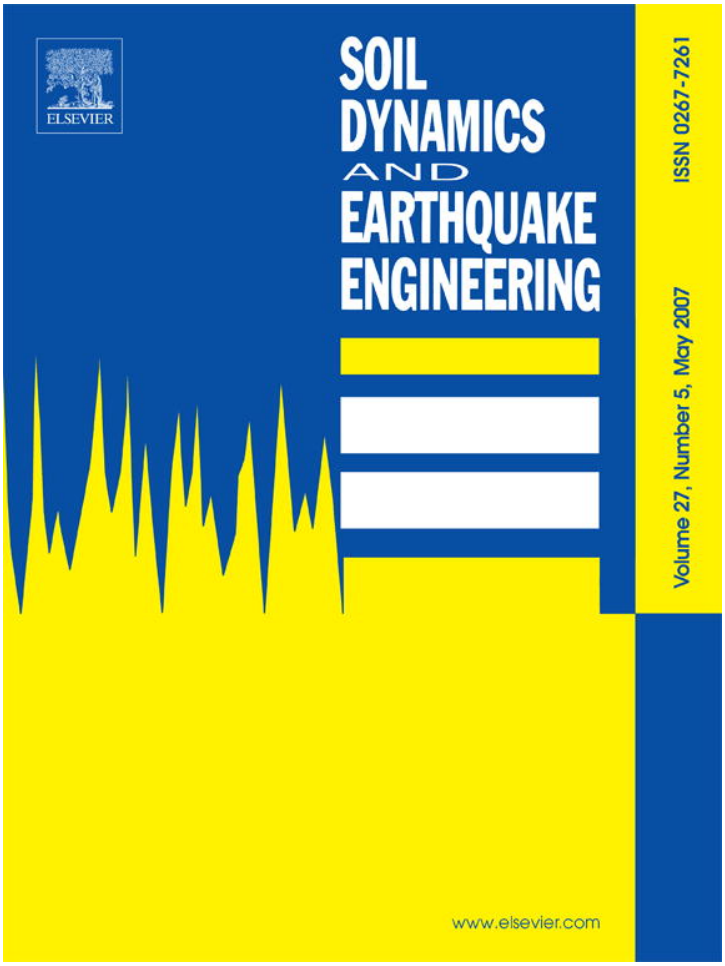

ELSEVIER

Soil Dynamics and Earthquake Engineering 27 (2007) 448–462

SOIL DYNAMICS AND EARTHQUAKE ENGINEERING

www.elsevier.com/locate/soildyn

Three-dimensional time-harmonic Green's functions of saturated soil under buried loading

S.L. Chen[a,*], L.Z. Chen[a], E. Pan[b,**]

[a]*Department of Civil Engineering, Shanghai Jiaotong University, 800 Dongchuan Road, Minhang, Shanghai, PR China*
[b]*Department of Civil Engineering, The University of Akron, Akron, OH 44325-3905, USA*

Received 5 July 2006; received in revised form 22 September 2006; accepted 25 September 2006

Abstract

Three-dimensional time-harmonic response of a poroelastic half space subjected to an arbitrary buried loading is investigated. The analysis starts with the field equations in cylindrical coordinates based on Biot's general theory of poroelasticity. General solutions for the displacements are first derived using the Fourier expansions and Hankel integral transform with respect to the circumferential and radial coordinates, respectively. The transformed-domain solutions are obtained in explicit form. The physical-domain displacements and stress components are then obtained numerically by inverse integral transform. Comparisons illustrating the accuracy of the developed approach are made with existing solutions for an elastic half space, which is reduced directly from the general solution developed in the paper. Numerical results are presented for the displacements of a saturated soil subjected to a horizontal internal excitation.

Keywords: Saturated soil; Lamb's problem; Three-dimensional; Time harmonic; Green's function; Integral transform

1. Introduction

The dynamic response of an elastic half space is of great interest in civil engineering because of its fundamental importance in dynamic soil–structure interaction, earthquake engineering, and foundation vibration. The original formulation of the problem was presented by Lamb [1], who studied the dynamic response of an elastic half space subjected to concentrated loads acting at the surface or inside the half-space (surface- and internal-source problems, respectively). Since then, the classical Lamb's problem has been extended to many different and complicated situations. Newlands [2] extended the Lamb's problem to include dissipation due to internal friction. Pekeris [3,4] gave exact closed-form solutions of displacements produced by surface and buried point pulses. Pak [5] derived the dynamic response of an elastic half space due to an arbitrary, time-harmonic, finite, and buried source using the method of potentials. While Rajapakse and Wang [6,7] investigated two-dimensional (2D) and three-dimensional (3D) elastodynamic Green's functions of a transversely isotropic medium under harmonic buried excitation, Wang and Achenbach [8] solved the Lamb's problem in anisotropic elastic half space.

Soils can be modeled as two-phase materials consisting of a solid skeleton with voids filled with water and thus should be more realistically regarded as poroelastic materials. The first theory of wave propagation in a fluid-saturated porous medium was established by Biot [9,10] based on his earlier work on quasistatic poroelasticity [11]. Biot [12,13] also extended his analysis to include cases in which the soil skeleton is an anisotropic elastic material or a viscoelastic material. Current development in this field can be found, for example, in [14–17].

*Corresponding author. Tel.: +86 21 5474 2702; fax: +86 21 5474 3044.
**Also to be corresponded to. Tel.: +1 330 972 6739; fax: +1 330 972 6020.
E-mail addresses: shengli_chen@sjtu.edu.cn (S.L. Chen), pan2@uakron.edu (E. Pan).

0267-7261/$ - see front matter © 2006 Elsevier Ltd. All rights reserved.
doi:10.1016/j.soildyn.2006.09.006

Many researchers have studied the dynamic response of poroelastic media based on the Biot's poroelasticity theory. Manolis and Beskos [18,19] presented an integral formulation of dynamic poroelasticity in the Laplace transformed domain. Their fundamental solutions are associated with wave propagation problems in unbounded poroelastic media. Simon et al. [20] studied the one-dimensional transient response of saturated porous elastic solids for the special situation where the solid and fluid materials are dynamically compatible. Paul [21,22] considered the poroelastic counterpart of the classical Lamb's problem for an impulsive line load (2D plane strain problem) applied at the surface by assuming nondissipative behavior. Halpern and Christiano [23] analyzed the response of poroelastic half space due to steady-state harmonic surface tractions and presented a methodology for the solution of mixed boundary-value problems. A similar problem was treated later on by Philippacopoulos [24], who obtained an analytical solution of the problem using four displacement potentials and the Fourier–Bessel integral representation. Senjuntichai and Rajapakse [25] presented a detailed study on the dynamic Green's functions of a poroelastic half space subjected to various buried loads, and recently, extended their work to the vertical vibration of a circular plate in multilayered poroelastic medium [26].

The above solutions [21–25] to the dynamic response in poroelastic media are restricted to the axisymmetric or plane strain cases, which involve only two spatial dimensions, and are mostly concerned with surface loading. In contrast, only a few investigations have been reported in the literature for the corresponding asymmetric buried source case. Recently, Philippacopoulos [27] and Jin [28] obtained the 3D dynamic response of a poroelastic half space for the simplest loading case, i.e., a buried point source. The approaches used by these authors, however, require prior knowledge of the corresponding Green's function for the full space. Zhou et al. [29] presented the transient solution of saturated soil to a concentrated impulsive loading by neglecting the inertia coupling between the solid skeleton and fluid and assuming incompressible constitutes. It is well known that 3D solutions corresponding to time-harmonic loading applied at a finite depth below the semi-infinite saturated soil have wide applications in geomechanics and earthquake engineering. General solutions for the 3D Green's functions of poroelastic half space to an arbitrary buried source, however, have not been reported in the literature.

The present paper is concerned with this problem. The procedure developed is of sufficient generality to cover a variety of axisymmetric and asymmetric problems. The analysis starts with the general field equations in cylindrical coordinates following Biot's theory. In particular, the compressibility of the soil skeleton and pore water has been taken into account. General solutions for the displacements and stress components of the saturated medium are obtained by using Fourier expansion and Hankel integral transform with respect to the circumferential and radial coordinates, respectively. These general solutions, with consideration of the boundary conditions, are then used to solve the 3D Lamb's problem of saturated soils corresponding to arbitrary loads applied at a finite depth below the surface. Explicit expressions for displacements are presented in terms of simple integrations, which can be reduced directly to the corresponding elastic solutions. As numerical examples, the displacement components in the vertical and radial directions in a semi-infinite saturated soil subjected to a horizontal internal excitation are presented.

2. Governing equations

Consider the model shown in Fig. 1. The semi-infinite saturated soil is subjected to an arbitrary time-harmonic buried load located at a horizontal plane $z = z'$ and over the area $\mathbf{\Pi}$, and its constitutive behavior follows Biot's two-phase linear theory. Assuming that the motion under consideration is time harmonic with a factor $e^{i\omega t}$, the governing differential equations for the saturated soil in the cylindrical coordinate system (r,θ,z), in terms of displacements, are given as

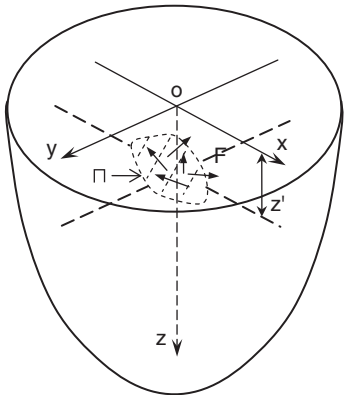

Fig. 1. Semi-infinite saturated soil under the action of arbitrary buried source.

follows [13,23,25]:

$$G(\nabla^2 u_r - \frac{1}{r^2}u_r - \frac{2}{r^2}\frac{\partial u_\theta}{\partial \theta}) + (\lambda + \alpha^2 M + G)\frac{\partial e}{\partial r} + \alpha M \frac{\partial \varepsilon}{\partial r} = -\rho\omega^2 u_r - \rho_w \omega^2 w_r, \tag{1a}$$

$$G(\nabla^2 u_\theta - \frac{1}{r^2}u_\theta + \frac{2}{r^2}\frac{\partial u_r}{\partial \theta}) + (\lambda + \alpha^2 M + G)\frac{\partial e}{r\partial \theta} + \alpha M \frac{\partial \varepsilon}{r\partial \theta} = -\rho\omega^2 u_\theta - \rho_w \omega^2 w_\theta, \tag{1b}$$

$$G\nabla^2 u_z + (\lambda + \alpha^2 M + G)\frac{\partial e}{\partial z} + \alpha M \frac{\partial \varepsilon}{\partial z} = -(\rho\omega^2 u_z + \rho_w \omega^2 w_z), \tag{1c}$$

$$\alpha M \frac{\partial e}{\partial r} + M \frac{\partial \varepsilon}{\partial r} = -\rho_w \omega^2 u_r - \vartheta\omega^2 w_r + \mathrm{i}b\omega w_r, \tag{1d}$$

$$\alpha M \frac{\partial e}{r\partial \theta} + M \frac{\partial \varepsilon}{r\partial \theta} = -\rho_w \omega^2 u_\theta - \vartheta\omega^2 u_\theta + \mathrm{i}b\omega u_\theta, \tag{1e}$$

$$\alpha M \frac{\partial e}{\partial z} + M \frac{\partial \varepsilon}{\partial z} = -\rho_w \omega^2 u_z - \vartheta\omega^2 w_z + \mathrm{i}b\omega w_z, \tag{1f}$$

in which u_r, u_θ, and u_z are radial, circumferential, and vertical displacements of the solid matrix, respectively; w_r, w_θ, and w_z are the average fluid displacements relative to the solid matrix in the r, θ, and z directions, respectively; e and ε are the matrix dilation and the fluid dilation relative to the solid, respectively, which are expressed as

$$e = \frac{\partial u_r}{\partial r} + \frac{u_r}{r} + \frac{\partial u_\theta}{r\partial \theta} + \frac{\partial u_z}{\partial z},\ \varepsilon = \frac{\partial w_r}{\partial r} + \frac{w_r}{r} + \frac{\partial w_\theta}{r\partial \theta} + \frac{\partial w_z}{\partial z}.$$

λ and G are Lame's constants of the solid matrix; α and M are, respectively, the Biot's compressibility parameters of skeletal frame and water; ρ_w is the mass density of water and ρ the mass density of bulk material ($\rho = n\rho_w + (1–n)\rho_s$, n = porosity and ρ_s = mass density of grains); ϑ is a density-like parameter that depends on ρ_w and geometry of the pores; b is a parameter accounting for the internal friction due to the relative motion between the solid matrix and the pore water, and is equal to the ratio between the fluid viscosity and the intrinsic permeability of the medium; ω is the circular frequency of motion and ∇^2 denotes the Laplacian operator which is given by

$$\nabla^2 = \frac{\partial^2}{\partial r^2} + \frac{1}{r}\frac{\partial}{\partial r} + \frac{1}{r^2}\frac{\partial^2}{\partial \theta^2} + \frac{\partial^2}{\partial z^2}.$$

For convenience, the time factor $e^{i\omega t}$ has been suppressed in Eqs. (1a)–(1f) and also in the sequel.

The constitutive relations for the z-direction traction components and pore pressure in the saturated soil can be expressed as

$$\sigma_z = 2G\frac{\partial u_z}{\partial z} + \lambda e, \tag{2a}$$

$$\tau_{zr} = G\left(\frac{\partial u_r}{\partial z} + \frac{\partial u_z}{\partial r}\right), \tag{2b}$$

$$\tau_{z\theta} = G\left(\frac{\partial u_z}{r\partial \theta} + \frac{\partial u_\theta}{\partial z}\right), \tag{2c}$$

$$\sigma_f = -\alpha M e - M\varepsilon, \tag{2d}$$

in which σ_z is the effective normal stress component in the vertical z-direction; τ_{zr}, $\tau_{z\theta}$ are shear stresses and σ_f denotes the excess pore pressure.

3. Solutions of governing equations

Using Fourier expansion with respect to the circumferential coordinate θ, the displacement and stress fields appearing in Eqs. (1) and (2) become [30]

$$u_r(r,\theta,z) = \sum_{m=0}^{\infty}[u_{rm,1}(r,z)\cos m\theta - u_{rm,2}(r,z)\sin m\theta], \tag{3a}$$

$$u_\theta(r,\theta,z)=\sum_{m=0}^{\infty}[u_{\theta m,1}(r,z)\ \sin\ m\theta+u_{\theta m,2}(r,z)\ \cos\ m\theta], \tag{3b}$$

$$u_z(r,\theta,z)=\sum_{m=0}^{\infty}[u_{zm,1}(r,z)\ \cos\ m\theta-u_{zm,2}(r,z)\ \sin\ m\theta], \tag{3c}$$

$$w_r(r,\theta,z)=\sum_{m=0}^{\infty}[w_{rm,1}(r,z)\ \cos\ m\theta-w_{rm,2}(r,z)\ \sin\ m\theta], \tag{3d}$$

$$w_\theta(r,\theta,z)=\sum_{m=0}^{\infty}[w_{\theta m,1}(r,z)\ \sin\ m\theta+w_{\theta m,2}(r,z)\ \cos\ m\theta], \tag{3e}$$

$$w_z(r,\theta,z)=\sum_{m=0}^{\infty}[w_{zm,1}(r,z)\ \cos\ m\theta-w_{zm,2}(r,z)\ \sin\ m\theta], \tag{3f}$$

$$\sigma_z(r,\theta,z)=\sum_{m=0}^{\infty}[\sigma_{zm,1}(r,z)\ \cos\ m\theta-\sigma_{zm,2}(r,z)\ \sin\ m\theta], \tag{3g}$$

$$\tau_{zr}(r,\theta,z)=\sum_{m=0}^{\infty}[\tau_{zrm,1}(r,z)\ \cos\ m\theta-\tau_{zrm,2}(r,z)\ \sin\ m\theta], \tag{3h}$$

$$\tau_{z\theta}(r,\theta,z)=\sum_{m=0}^{\infty}[\tau_{z\theta m,1}(r,z)\ \sin\ m\theta+\tau_{z\theta m,2}(r,z)\ \cos\ m\theta], \tag{3i}$$

$$\sigma_f=\sum_{m=0}^{\infty}[\sigma_{fm,1}\ \cos\ m\theta-\sigma_{fm,2}\ \sin\ m\theta], \tag{3j}$$

$$e=\sum_{m=0}^{\infty}[e_{m,1}\ \cos\ m\,\theta-e_{m,2}\ \sin\ m\theta], \tag{3k}$$

$$\varepsilon=\sum_{m=0}^{\infty}[\varepsilon_{m,1}\ \cos\ m\theta-\varepsilon_{m,2}\ \sin\ m\theta], \tag{3l}$$

where for $k=1, 2$,

$$e_{m,k}=\frac{\partial u_{rm,k}}{\partial r}+\frac{u_{rm,k}}{r}+\frac{m}{r}u_{\theta m,k}+\frac{\partial u_{zm,k}}{\partial z}$$

and

$$\varepsilon_{m,k}=\frac{\partial w_{rm,k}}{\partial r}+\frac{w_{rm,k}}{r}+\frac{m}{r}w_{\theta m,k}+\frac{\partial w_{zm,k}}{\partial z}.$$

Substituting Eq. (3) into Eqs. (1) and (2) and further defining the operator

$$\nabla_m^2=\frac{\partial^2}{\partial r^2}+\frac{1}{r}\frac{\partial}{\partial r}-\frac{m^2}{r^2}+\frac{\partial^2}{\partial z^2},$$

one obtains the following equations for $k=1, 2$ and $m=0, 1, 2, \ldots$:

$$G(\nabla_m^2-\frac{1}{r^2})u_{rm,k}-\frac{2Gm}{r^2}u_{\theta m,k}+(\lambda+\alpha^2M+G)\frac{\partial e_{m,k}}{\partial r}+\alpha M\frac{\partial \varepsilon_{m,k}}{\partial r}=-\rho\omega^2u_{rm,k}-\rho_w\omega^2w_{rm,k}, \tag{4a}$$

$$-\frac{2Gm}{r^2}u_{rm,k}+G(\nabla_m^2-\frac{1}{r^2})u_{\theta m,k}-(\lambda+\alpha^2M+G)\frac{me_{m,k}}{r}-\frac{\alpha Mm}{r}\varepsilon_{m,k}=-\rho\omega^2u_{\theta m,k}-\rho_w\omega^2w_{\theta m,k}, \tag{4b}$$

$$G\nabla_m^2u_{zm,k}+(\lambda+\alpha^2M+G)\frac{\partial e_{m,k}}{\partial z}+\alpha M\frac{\partial \varepsilon_{m,k}}{\partial z}=-\rho\omega^2u_{zm,k}-\rho_w\omega^2w_{zm,k}, \tag{4c}$$

$$\alpha M\frac{\partial e_{m,k}}{\partial r}+M\frac{\partial \varepsilon_{m,k}}{\partial r}=-\rho_{\mathrm{w}}\omega^2u_{rm,k}-\vartheta\omega^2w_{rm,k}+\mathrm{i}b\omega w_{rm,k}, \tag{4d}$$

$$-\alpha M\frac{me_{m,k}}{r}-Mm\frac{\varepsilon_{m,k}}{r}=-\rho_{\mathrm{w}}\omega^2u_{\theta m,k}-\vartheta\omega^2w_{\theta m,k}+\mathrm{i}b\omega w_{\theta m,k}, \tag{4e}$$

$$\alpha M\frac{\partial e_{m,k}}{\partial z}+M\frac{\partial \varepsilon_{m,k}}{\partial z}=-\rho_{\mathrm{w}}\omega^2u_{zm,k}-\vartheta\omega^2w_{zm,k}+\mathrm{i}b\omega w_{zm,k}. \tag{4f}$$

$$\sigma_{zm}=2G\frac{\partial u_{zm,k}}{\partial z}+\lambda e_{m,k}, \tag{5a}$$

$$\tau_{zrm,k}=G\left(\frac{\partial u_{rm,k}}{\partial z}+\frac{\partial u_{zm,k}}{\partial r}\right), \tag{5b}$$

$$\tau_{z\theta m,k}=G\left(-\frac{mu_{zm,k}}{r}+\frac{\partial u_{\theta m,k}}{\partial z}\right), \tag{5c}$$

$$\sigma_{fm,k}=-\alpha Me_{m,k}-M\varepsilon_{m,k}. \tag{5d}$$

Performing $(\partial/\partial r)$ Eq. (4a) $+(1/r)$ Eq. (4a) $+(m/r)$ Eq. (4b) $+(\partial/\partial z)$ Eq. (4c), and $(\partial/\partial r)$ Eq. (4d) $+(1/r)$ Eq. (4d) $+(m/r)$ Eq. (4e) $+(\partial/\partial z)$ Eq. (4f), we finally obtain

$$(\lambda+2G+\alpha^2M)\nabla_m^2e_{m,k}+\alpha M\nabla_m^2\varepsilon_{m,k}=-\rho\omega^2e_{m,k}-\rho_{\mathrm{w}}\omega^2\varepsilon_{m,k}, \tag{6}$$

$$\alpha M\nabla_m^2e_{m,k}+M\nabla_m^2\varepsilon_{m,k}=-\rho_{\mathrm{w}}\omega^2e_{m,k}+(\mathrm{i}b\omega-\vartheta\omega^2)\varepsilon_{m,k}. \tag{7}$$

The μth Hankel transform with respect to r is defined as

$$\tilde{f}^{\mu}(p)=H^{\mu}[f]=\int_0^{\infty}rf(r)J_{\mu}(rp)\mathrm{d}r, \tag{8a}$$

$$f(r)=\int_0^{\infty}p\tilde{f}^{\mu}(p)J_{\mu}(rp)\mathrm{d}p, \tag{8b}$$

where p is the parameter for the Hankel transform and J_{μ} denotes the Bessel function of the first kind of order μ.

Application of the mth order Hankel transform to Eqs. (6) and (7) then results in

$$(\lambda_c+2G)\frac{\mathrm{d}^2}{\mathrm{d}z^2}\tilde{e}_{m,k}^m+[\rho\omega^2-(\lambda_c+2G)p^2]\tilde{e}_{m,k}^m=-\alpha M\frac{\mathrm{d}^2}{\mathrm{d}z^2}\tilde{\varepsilon}_{m,k}^m+(\alpha Mp^2-\rho_{\mathrm{w}}\omega^2)\tilde{\varepsilon}_{m,k}^m, \tag{9}$$

$$\alpha M\frac{\mathrm{d}^2}{\mathrm{d}z^2}\tilde{e}_{m,k}^m+(\rho_{\mathrm{w}}\omega^2-\alpha Mp^2)\tilde{e}_{m,k}^m=-M\frac{\mathrm{d}^2}{\mathrm{d}z^2}\tilde{\varepsilon}_{m,k}^m+(Mp^2+\mathrm{i}b\omega-\vartheta\omega^2)\tilde{\varepsilon}_{m,k}^m, \tag{10}$$

where $\lambda_c=\lambda+\alpha^2M$. Eqs. (9) and (10) can be solved directly and the results can be expressed as

$$\tilde{e}_{m,k}^m=-p_1^2A_{1m,k}\mathrm{e}^{-cz}-p_1^2A_{2m,k}\mathrm{e}^{cz}-p_2^2B_{1m,k}\mathrm{e}^{-dz}-p_2^2B_{2m,k}\mathrm{e}^{dz}, \tag{11}$$

$$\tilde{\varepsilon}_{m,k}^m=-p_1^2\delta_1(A_{1m,k}\mathrm{e}^{-cz}+A_{2m,k}\mathrm{e}^{cz})-p_2^2\delta_2(B_{1m,k}\mathrm{e}^{-dz}+B_{2m,k}\mathrm{e}^{dz}), \tag{12}$$

in which $c=\sqrt{p^2-p_1^2}$, $d=\sqrt{p^2-p_2^2}$, p_1, p_2 are the complex wave numbers associated with the dilatational waves of the first and second kind, respectively, given by $p_1^2=(\beta_1+\sqrt{\beta_1^2-4\beta_2})/2$ and $p_2^2=(\beta_1-\sqrt{\beta_1^2-4\beta_2})/2$, $\beta_1=[(\lambda_c+2G)(\vartheta\omega^2-\mathrm{i}b\omega)-2\alpha M\rho_{\mathrm{w}}\omega^2+M\rho\omega^2]/(\lambda+2G)M$, $\beta_2=[(\vartheta\omega^2-\mathrm{i}b\omega)\rho\omega^2-\rho_w^2\omega^4]/(\lambda+2G)M$, and c and d are so selected that $\mathrm{Re}[c]\geqslant 0$, $\mathrm{Re}[d]\geqslant 0$; $\delta_1=[(\lambda_c+2G)p_1^2-\rho\omega^2]/(\rho_{\mathrm{w}}\omega^2-\alpha Mp_1^2)$, $\delta_2=[(\lambda_c+2G)p_2^2-\rho\omega^2]/(\rho_{\mathrm{w}}\omega^2-\alpha Mp_2^2)$; $A_{1m,k}$, $A_{2m,k}$, $B_{1m,k}$, and $B_{2m,k}$ are arbitrary functions of p and z.

Substitution of Eqs. (11) and (12) back into Eqs. (4c) and (4f) thus yields the following solutions for the vertical displacements:

$$\tilde{u}_{zm,k}^m=-c(A_{1m,k}\mathrm{e}^{-cz}-A_{2m,k}\mathrm{e}^{cz})-d(B_{1m,k}\mathrm{e}^{-dz}-B_{2m,k}\mathrm{e}^{dz})+p^2(R_{1m,k}\mathrm{e}^{-jz}+R_{2m,k}\mathrm{e}^{jz}), \tag{13}$$

$$\tilde{w}_{zm,k}^m=-c\delta_1(A_{1m,k}\mathrm{e}^{-cz}-A_{2m,k}\mathrm{e}^{cz})-d\delta_2(B_{1m,k}\mathrm{e}^{-dz}-B_{2m,k}\mathrm{e}^{dz})+p^2\delta_3(R_{1m,k}\mathrm{e}^{-jz}+R_{2m,k}\mathrm{e}^{jz}), \tag{14}$$

in which $j=\sqrt{p^2-s^2}$, $s^2=[\rho\omega^2(\mathrm{i}b\omega-\vartheta\omega^2)+\rho_{\mathrm{w}}^2\omega^4]/G(\mathrm{i}b\omega-\vartheta\omega^2)$, s is the complex wave number associated with the rotational wave and is again selected such that $\mathrm{Re}[s]\geqslant 0$; $\delta_3=\rho_{\mathrm{w}}\omega^2/(\mathrm{i}b\omega-\vartheta\omega^2)$; $R_{1m,k}$, $R_{2m,k}$ are also arbitrary functions of p and z.

Adding Eq. (4a) to (4b) and Eq. (4d) to (4e), and then applying the $(m+1)$th Hankel transform to the resulting equations gives

$$G\frac{\mathrm{d}^2}{\mathrm{d}z^2}\{H^{m+1}[u_{rm,k}+u_{\theta m,k}]\}+(\rho\omega^2-Gp^2)H^{m+1}[u_{rm,k}+u_{\theta m,k}]=-\rho_{\mathrm{w}}\omega^2H^{m+1}[w_{rm,k}+w_{\theta m,k}]+(\lambda_c+G)p\tilde{e}^m_{m,k}+\alpha Mp\tilde{\varepsilon}^m_{m,k}, \tag{15}$$

$$H^{m+1}[w_{rm,k}+w_{\theta m,k}]=\frac{1}{\mathrm{i}b\omega-\vartheta\omega^2}\left\{\rho_{\mathrm{w}}\omega^2H^{m+1}[u_{rm,k}+u_{\theta m,k}]-\alpha Mp\tilde{e}^m_{m,k}-Mp\tilde{\varepsilon}^m_{m,k}\right\}. \tag{16}$$

Similarly, subtraction of Eq. (4b) from (4a) and Eq. (4e) from (4d), followed by the application of the $(m-1)$th Hankel transform, gives

$$G\frac{\mathrm{d}^2}{\mathrm{d}z^2}\{H^{m-1}[u_{rm,k}-u_{\theta m,k}]\}+(\rho\omega^2-Gp^2)H^{m-1}[u_{rm,k}-u_{\theta m,k}]=-\rho_{\mathrm{w}}\omega^2H^{m-1}[w_{rm,k}-w_{\theta m,k}]-(\lambda_c+G)p\tilde{e}^m_{m,k}-\alpha Mp\tilde{\varepsilon}^m_{m,k}, \tag{17}$$

$$H^{m-1}[w_{rm,k}-w_{\theta m,k}]=\frac{1}{\mathrm{i}b\omega-\vartheta\omega^2}\left\{\rho_{\mathrm{w}}\omega^2H^{m-1}[u_{rm,k}-u_{\theta m,k}]+\alpha Mp\tilde{e}^m_{m,k}+Mp\tilde{\varepsilon}^m_{m,k}\right\}. \tag{18}$$

The solutions of Eqs (15)–(18) can easily be found to be

$$H^{m+1}[u_{rm,k}+u_{\theta m,k}]=-p(A_{1m,k}\mathrm{e}^{-cz}+A_{2m,k}\mathrm{e}^{cz})-p(B_{1m,k}\mathrm{e}^{-dz}+B_{2m,k}\mathrm{e}^{dz})+2pj(T_{1m,k}\mathrm{e}^{-jz}+T_{2m,k}\mathrm{e}^{jz}), \tag{19}$$

$$\mathrm{H}^{m+1}[w_{rm,k}+w_{\theta m,k}]=-p\delta_1(A_{1m,k}\mathrm{e}^{-cz}+A_{2m,k}\mathrm{e}^{cz})-p\delta_2(B_{1m,k}\mathrm{e}^{-dz}+B_{2m,k}\mathrm{e}^{dz})+2pj\delta_3(T_{1m,k}\mathrm{e}^{-jz}+T_{2m,k}\mathrm{e}^{jz}), \tag{20}$$

$$\mathrm{H}^{m-1}[u_{rm,k}-u_{\theta m,k}]=p(A_{1m,k}\mathrm{e}^{-cz}+A_{2m,k}\mathrm{e}^{cz})+p(B_{1m,k}\mathrm{e}^{-dz}+B_{2m,k}\mathrm{e}^{dz})+2pj[(T_{1m,k}-R_{1m,k})\mathrm{e}^{-jz}+(T_{2m,k}+R_{2m,k})\mathrm{e}^{jz}], \tag{21}$$

$$\mathrm{H}^{m-1}[w_{rm,k}-w_{\theta m,k}]=p\delta_1(A_{1m,k}\mathrm{e}^{-cz}+A_{2m,k}\mathrm{e}^{cz})+p\delta_2(B_{1m,k}\mathrm{e}^{-dz}+B_{2m,k}\mathrm{e}^{dz})+2pj\delta_3[(T_{1m,k}-R_{1m,k})\mathrm{e}^{-jz}+(T_{2m,k}+R_{2m,k})\mathrm{e}^{jz}], \tag{22}$$

in which $T_{1m,k}$ and $T_{2m,k}$ are arbitrary functions of p and z.

Next, the expressions for stresses of the solid matrix and pore water can be obtained straightforwardly by combining Eqs. (5a)–(5d) with Eqs. (11)–(13), (19), and (21) as follows:

$$\tilde{\sigma}^m_{zm,k}=k_1(A_{1m,k}e^{-cz}+A_{2m,k}e^{cz})+k_2(B_{1m,k}\mathrm{e}^{-dz}+B_{2m,k}\mathrm{e}^{dz})-2Gp^2j(R_{1m,k}\mathrm{e}^{-jz}-R_{2m,k}\mathrm{e}^{jz}), \tag{23}$$

$$\mathrm{H}^{m+1}[\tau_{zrm,k}+\tau_{z\theta m,k}]=2pcG(A_{1m,k}\mathrm{e}^{-cz}-A_{2m,k}\mathrm{e}^{cz})+2pdG(B_{1m,k}\mathrm{e}^{-dz}-B_{2m,k}\mathrm{e}^{dz})+pG[-(p^2R_{1m,k}+2j^2T_{1m,k})\mathrm{e}^{-jz}+(2j^2T_{2m,k}-p^2R_{2m,k})\mathrm{e}^{jz}], \tag{24}$$

$$H^{m-1}[\tau_{zrm,k}-\tau_{z\theta m,k}]=-2pcG(A_{1m,k}\mathrm{e}^{-cz}-A_{2m,k}\mathrm{e}^{cz})-2pdG(B_{1m,k}\mathrm{e}^{-dz}-B_{2m,k}\mathrm{e}^{dz})+pG[(p^2R_{1m,k}+2j^2R_{1m,k}-2j^2T_{1m,k})\mathrm{e}^{-jz}+(p^2R_{2m,k}+2j^2R_{2m,k}+2j^2T_{2m,k})\mathrm{e}^{jz}], \tag{25}$$

$$\tilde{\sigma}^m_{fm,k}=a_1(A_{1m,k}\mathrm{e}^{-cz}+A_{2m,k}\mathrm{e}^{cz})+a_2(B_{1m,k}\mathrm{e}^{-dz}+B_{2m,k}\mathrm{e}^{dz}), \tag{26}$$

in which $k_1=(\lambda+2G)c^2-\lambda p^2$, $k_2=(\lambda+2G)d^2-\lambda p^2$; $a_1=(\alpha+\delta_1)Mp_1^2$ and $a_2=(\alpha+\delta_2)Mp_2^2$.

In summary, the Fourier components of the displacements and stresses for the solid matrix and the pore water pressure have been obtained in the Hankel transform domain. The eight unknown functions $A_{1m,k}$, $A_{2m,k}$, $B_{1m,k}$, $B_{2m,k}$, $R_{1m,k}$, $R_{2m,k}$, $T_{1m,k}$, and $T_{2m,k}$ can be determined from the boundary conditions at the free surface of the half space and the continuity conditions at a fictitious horizontal plane passing through the source level.

4. Boundary conditions

Let us consider the boundary-value problem of a semi-infinite saturated soil subjected to an internal source. As shown in Fig. 1, the surface of the saturated soil is assumed to be a drainage boundary and a time-harmonic, arbitrary distributed buried load $\mathbf{F}(r,\theta,z)=f_r(r,\theta,z')\delta(z-z')\mathbf{e}_r+f_\theta(r,\theta,z')\delta(z-z')\mathbf{e}_\theta+f_z(r,\theta,z')\delta(z-z')\mathbf{e}_z$ is applied at a horizontal plane $z=z'$. Following the Pekeris approach which is also employed by Pak [5] and Senjuntichai and Rajapakse [25], the half

space is treated as a two-domain problem across a fictitious plane at $z = z'$. The upper region bounded by $0 \leqslant z \leqslant z'$ is defined as domain 1 whilst the lower region bounded by $z \leqslant z' \leqslant \infty$ as domain 2. In what follows, the superscripts (1) and (2) are used to denote quantities associated with these two domains. It is evident that the four arbitrary functions $A^{(2)}_{2m,k}$, $B^{(2)}_{2m,k}$, $R^{(2)}_{2m,k}$ and $T^{(2)}_{2m,k}$ corresponding to domain 2 must vanish to guarantee the regularity of solution at infinity. The boundary conditions at the surface $z = 0$ and the interface conditions at the fictitious plane $z = z'$ can be written as follows:

$$\sigma^{(1)}_{zm,k}(r,0) = 0, \tag{27a}$$

$$\tau^{(1)}_{zrm,k}(r,0) = 0, \tag{27b}$$

$$\tau^{(1)}_{z\theta m,k}(r,0) = 0, \tag{27c}$$

$$\sigma^{(1)}_{fm,k}(r,0) = 0, \tag{27d}$$

$$u^{(1)}_{zm,k}(r,z') - u^{(2)}_{zm,k}(r,z') = 0, \tag{27e}$$

$$\left[u^{(1)}_{rm,k}(r,z') + u^{(1)}_{\theta m,k}(r,z')\right] - \left[u^{(2)}_{rm,k}(r,z') + u^{(2)}_{\theta m,k}(r,z')\right] = 0, \tag{27f}$$

$$\left[u^{(1)}_{rm,k}(r,z') - u^{(1)}_{\theta m,k}(r,z')\right] - \left[u^{(2)}_{rm,k}(r,z') - u^{(2)}_{\theta m,k}(r,z')\right] = 0, \tag{27g}$$

$$\sigma^{(1)}_{fm,k}(r,z') - \sigma^{(2)}_{fm,k}(r,z') = 0, \tag{27h}$$

$$\sigma^{(1)}_{zm,k}(r,z') - \sigma^{(2)}_{zm,k}(r,z') = f_{zm,k}(r,z'), \tag{27i}$$

$$\left[\tau^{(1)}_{zrm,k}(r,z') + \tau^{(1)}_{z\theta m,k}(r,z')\right] - \left[\tau^{(2)}_{zrm,k}(r,z') + \tau^{(2)}_{z\theta m,k}(r,z')\right] = f_{rm,k}(r,z') + f_{\theta m,k}(r,z'), \tag{27j}$$

$$\left[\tau^{(1)}_{zrm,k}(r,z') - \tau^{(1)}_{z\theta m,k}(r,z')\right] - \left[\tau^{(2)}_{zrm,k}(r,z') - \tau^{(2)}_{z\theta m,k}(r,z')\right] = f_{rm,k}(r,z') - f_{\theta m,k}(r,z'), \tag{27k}$$

$$w^{(1)}_{zm,k}(r,z') - w^{(2)}_{zm,k}(r,z') = 0, \tag{27l}$$

in which $f_{rm,k}(r,z')$, $f_{\theta m,k}(r,z')$ and $f_{zm,k}(r,z')$ are the Fourier coefficients of the loading distributions $f_r(r,\theta,z')$, $f_\theta(r,\theta,z')$ and $f_z(r,\theta,z')$, respectively, and satisfy the relations

$$f_r(r,\theta,z') = \sum_{m=0}^{\infty}[f_{rm,1}(r,z')\cos m\theta - f_{rm,2}(r,z')\sin m\theta], \tag{28a}$$

$$f_\theta(r,\theta,z') = \sum_{m=0}^{\infty}[f_{\theta m,1}(r,z')\sin m\theta + f_{\theta m,2}(r,z')\cos m\theta], \tag{28b}$$

$$f_z(r,\theta,z') = \sum_{m=0}^{\infty}[f_{zm,1}(r,z')\cos m\theta - f_{zm,2}(r,z')\sin m\theta]. \tag{28c}$$

On application of appropriate Hankel transforms to Eqs. (27a)–(27l) and after substitution of Eqs. (13), (14), (19), (21), and (23)–(26), one can rearrange the boundary conditions as

$$\mathbf{AX} = \mathbf{B}, \tag{29}$$

in which

$$\mathbf{X}^{\mathrm{T}} = \Big\{A^{(1)}_{1m,k}e^{-cz'}, A^{(1)}_{2m,k}e^{cz'}, B^{(1)}_{1m,k}e^{-dz'}, B^{(1)}_{2m,k}e^{dz'}, R^{(1)}_{1m,k}e^{-jz'}, R^{(1)}_{2m,k}e^{jz'}, T^{(1)}_{1m,k}e^{-jz'}, T^{(1)}_{2m,k}e^{jz'}, A^{(2)}_{1m,k}e^{-cz'}, B^{(2)}_{1m,k}e^{-dz'}, R^{(2)}_{1m,k}e^{-jz'}, T^{(2)}_{1m,k}e^{-jz'}\Big\}$$

and

$$\mathbf{B} = \Big\{0,0,0,0,0,0,0,0,\tilde{f}^{m}_{zm,k}(p,z'),\tilde{f}_{(r+\theta)m,k}(p,z'),\tilde{f}_{(r-\theta)m,k}(p,z'),0\Big\},$$

with

$$\tilde{f}_{(r+\theta)m,k}(p,z') = \frac{1}{Gp}\left\{H^{m+1}[f_{rm,k}(r,z') + f_{\theta m,k}(r,z')] + H^{m-1}[f_{rm,k}(r,z') - f_{\theta m,k}(r,z')]\right\}, \tilde{f}_{(r-\theta)m,k}(p,z') = \frac{1}{2Gp}\left\{H^{m+1}[f_{rm,k}(r,z') + f_{\theta m,k}(r,z')] - H^{m-1}[f_{rm,k}(r,z') - f_{\theta m,k}(r,z')]\right\},$$

and

$$\mathbf{A} = \begin{bmatrix} k_1 e^{cz'} & k_1 e^{-cz'} & k_2 e^{dz'} & k_2 e^{-dz'} & 2Gp^2 j e^{jz'} & 2Gp^2 j e^{-jz'} & 0 & 0 & 0 & 0 & 0 & 0 \\ a_1 e^{cz'} & a_1 e^{-cz'} & a_2 e^{dz'} & a_2 e^{-dz'} & 0 & 0 & 0 & 0 & 0 & 0 & 0 & 0 \\ 0 & 0 & 0 & 0 & e^{jz'} & e^{-jz'} & -2e^{jz'} & 2e^{-jz'} & 0 & 0 & 0 & 0 \\ 2ce^{cz'} & -2ce^{-cz'} & 2de^{dz'} & 2de^{-dz'} & -(p^2+j^2)e^{jz'} & -(p^2+j^2)e^{-jz'} & 0 & 0 & 0 & 0 & 0 & 0 \\ -c & c & -d & d & p^2 & p^2 & 0 & 0 & c & d & -p^2 & 0 \\ 0 & 0 & 0 & 0 & -2j & 2j & 4j & 4j & 0 & 0 & 2j & -4j \\ 1 & 1 & 1 & 1 & -j & -j & 0 & 0 & -1 & -1 & j & 0 \\ a_1 & a_1 & a_2 & a_2 & 0 & 0 & 0 & 0 & -a_1 & -a_2 & 0 & 0 \\ k_1 & k_1 & k_2 & k_2 & -2Gp^2 j & 2Gp^2 j & 0 & 0 & -k_1 & -k_2 & 2Gp^2 j & 0 \\ 0 & 0 & 0 & 0 & 2j^2 & 2j^2 & -4j^2 & 4j^2 & 0 & 0 & -2j^2 & 4j^2 \\ 2c & -2c & 2d & -2d & -(p^2+j^2) & -(p^2+j^2) & 0 & 0 & -2c & -2d & p^2+j^2 & 0 \\ -c\delta_1 & c\delta_1 & -d\delta_2 & d\delta_2 & p^2\delta_3 & p^2\delta_3 & 0 & 0 & c\delta_1 & d\delta_2 & -p^2\delta_3 & 0 \end{bmatrix}.$$

After lengthy but rather straightforward algebra, the solution of Eq. (29) can be shown explicitly as (via inverse of the above 12×12 nonsymmetric matrix)

$$A^{(1)}_{1m,k} = \frac{a_2 p^2 d f_2 e^{-cz'} - 8p^4 cdjGa_1 a_2 e^{-dz'} + 4Gcdjp^2 a_2(a_1-a_2)(2p^2-s^2)e^{-jz'}}{2s^2(a_1-a_2)cdf}\tilde{f}_{(r-\theta)m,k} + \frac{a_2 f_2 e^{-cz'} - 8p^2 djGa_1 a_2 e^{-dz'} + 4Gp^2 a_2(a_1-a_2)(2p^2-s^2)e^{-jz'}}{2Gs^2(a_1-a_2)f}\tilde{f}^m_{zm,k}, \tag{30a}$$

$$A^{(1)}_{2m,k} = \frac{a_2 p^2 e^{-cz'}}{2s^2 c(a_1-a_2)}\tilde{f}_{(r-\theta)m,k} + \frac{a_2 e^{-cz'}}{2Gs^2(a_1-a_2)}\tilde{f}^m_{zm,k}, \tag{30b}$$

$$B^{(1)}_{1m,k} = \frac{-8p^4 jGda_1 a_2 e^{-cz'} + a_1 f_1 p^2 e^{-dz'} - 4Gp^2 dja_1(a_1-a_2)(2p^2-s^2)e^{-jz'}}{2s^2(a_1-a_2)df}\tilde{f}_{(r-\theta)m,k} + \frac{-8p^2 jGca_1 a_2 e^{-cz'} + a_1 f_1 e^{-dz'} - 4Gp^2 a_1(a_1-a_2)(2p^2-s^2)e^{-jz'}}{2Gs^2(a_1-a_2)f}\tilde{f}^m_{zm,k}, \tag{30c}$$

$$B^{(1)}_{2m,k} = \frac{-p^2 a_1 e^{-dz'}}{2s^2 d(a_1-a_2)}\tilde{f}_{(r-\theta)m,k} - \frac{a_1 e^{-dz'}}{2Gs^2(a_1-a_2)}\tilde{f}^m_{zm,k}, \tag{30d}$$

$$R^{(1)}_{1m,k} = \frac{-4a_2 p^2 G(2p^2-s^2)e^{-cz'} + 4a_1 p^2 G(2p^2-s^2)e^{-dz'} - f_3 e^{-jz'}}{2s^2 f}\tilde{f}_{(r-\theta)m,k} + \frac{-4ca_2 jG(2p^2-s^2)e^{-cz'} + 4da_1 jG(2p^2-s^2)e^{-dz'} - f_3 e^{-jz'}}{2Gjs^2 f}\tilde{f}^m_{zm,k}, \tag{30e}$$

$$R^{(1)}_{2m,k} = \frac{e^{-jz'}}{2s^2}\tilde{f}_{(r-\theta)m,k} + \frac{e^{-jz'}}{2Gjs^2}\tilde{f}^m_{zm,k}, \tag{30f}$$

$$T^{(1)}_{1m,k} = \frac{1}{2}R^{(1)}_{1m,k} + \frac{e^{-jz'}}{8j^2}\tilde{f}_{(r+\theta)m,k}, \tag{30g}$$

$$T^{(1)}_{2m,k} = -\frac{1}{2}R^{(1)}_{2m,k} + \frac{e^{-jz'}}{8j^2}\tilde{f}_{(r+\theta)m,k}, \tag{30h}$$

$$A^{(2)}_{1m,k} = A^{(1)}_{1m,k} - A^{(1)}_{2m,k}\mathrm{e}^{2cz'} + \frac{p^2(\delta_2-\delta_3)}{cs^2(\delta_1-\delta_2)}\mathrm{e}^{cz'}\tilde{f}_{(r-\theta)m,k}, \tag{30i}$$

$$B^{(2)}_{1m,k} = B^{(1)}_{1m,k} - B^{(1)}_{2m,k}\mathrm{e}^{2dz'} - \frac{p^2(\delta_1-\delta_3)}{ds^2(\delta_1-\delta_2)}\mathrm{e}^{dz'}\tilde{f}_{(r-\theta)m,k}, \tag{30j}$$

$$R^{(2)}_{1m,k} = R^{(1)}_{1m,k} + R^{(1)}_{2m,k}\mathrm{e}^{2jz'} - \frac{1}{s^2}\mathrm{e}^{jz'}\tilde{f}_{(r-\theta)m,k}, \tag{30k}$$

$$T^{(2)}_{1m,k} = T^{(1)}_{1m,k} - T^{(1)}_{2m,k}\mathrm{e}^{2jz'} + \frac{1}{4j^2}\mathrm{e}^{jz'}\tilde{f}_{(r+\theta)m,k} - \frac{1}{2s^2}\mathrm{e}^{jz'}\tilde{f}_{(r-\theta)m,k}, \tag{30l}$$

where

$$f = G(a_1-a_2)(p^2+j^2)^2 - 4p^2jG(da_1-ca_2), \tag{31a}$$

$$f_1 = G(a_1-a_2)(p^2+j^2)^2 + 4p^2jG(da_1+ca_2), \tag{31b}$$

$$f_2 = -G(a_1-a_2)(p^2+j^2)^2 + 4p^2jG(da_1-ca_2), \tag{31c}$$

$$f_3 = G(a_1-a_2)(p^2+j^2)^2 + 4p^2jG(da_1-ca_2). \tag{31d}$$

Once the twelve unknown functions are obtained, the complete solution for the displacements, stresses, and pore water pressure corresponding to an arbitrary buried source can be obtained by substituting the arbitrary functions $A^{(1)}_{1m,k}$ to $T^{(2)}_{1m,k}$ into Eqs. (13), (14), and (19)–(26), then taking the respective inverse Hankel transforms, and finally summing them up with respect to m. In the following, we demonstrate this procedure for the solid displacements. The general expressions for the displacements in each domain ($i = 1,2$) are

$$u^{(i)}_r(r,\theta,z) = \frac{1}{2}\sum_{m=0}^{\infty}\sum_{k=1}^{2}\left\{\int_0^{\infty}\left[-p(A^{(i)}_{1m,k}\mathrm{e}^{-cz} + A^{(i)}_{2m,k}\mathrm{e}^{cz}) - p(B^{(i)}_{1m,k}\mathrm{e}^{-dz} + B^{(i)}_{2m,k}\mathrm{e}^{dz}) + 2pj(T^{(i)}_{1m,k}\mathrm{e}^{-jz} + T^{(i)}_{2m,k}\mathrm{e}^{jz})\right]\right.$$
$$\left.\times pJ_{m+1}(pr)\mathrm{d}p\right\}\cos\left[m\theta + \frac{k-1}{2}\pi\right] + \frac{1}{2}\sum_{m=0}^{\infty}\sum_{k=0}^{2}\left\{\int_0^{\infty}\left[p(A^{(i)}_{1m,k}\mathrm{e}^{-cz} + A^{(i)}_{2m,k}\mathrm{e}^{cz}) + p(B^{(i)}_{1m,k}\mathrm{e}^{-dz} + \right.\right.$$
$$\left.\left.B^{(i)}_{2m,k}e^{dz}) + 2pj\{(T^{(i)}_{1m,k} - R^{(i)}_{1m,k})\mathrm{e}^{-jz} + (T^{(i)}_{2m,k} + R^{(i)}_{2m,k})\mathrm{e}^{jz}\}\right]pJ_{m-1}(pr)\mathrm{d}p\right\}\cos\left[m\theta + \frac{k-1}{2}\pi\right], \tag{32}$$

$$u^{(i)}_\theta(r,\theta,z) = \frac{1}{2}\sum_{m=0}^{\infty}\sum_{k=1}^{2}\left\{\int_0^{\infty}\left[-p(A^{(i)}_{1m,k}\mathrm{e}^{-cz} + A^{(i)}_{2m,k}\mathrm{e}^{cz}) - p(B^{(i)}_{1m,k}\mathrm{e}^{-dz} + B^{(i)}_{2m,k}\mathrm{e}^{dz}) + 2pj(T^{(i)}_{1m,k}\mathrm{e}^{-jz} + T^{(i)}_{2m,k}\mathrm{e}^{jz})\right]\right.$$
$$\left.pJ_{m+1}(pr)\mathrm{d}p\right\}\cos\left[m\theta - \frac{k-1}{2}\pi\right] - \frac{1}{2}\sum_{m=0}^{\infty}\sum_{k=1}^{2}\left\{\int_0^{\infty}\left[p(A^{(i)}_{1m,k}\mathrm{e}^{-cz} + A^{(i)}_{2m,k}\mathrm{e}^{cz}) + p(B^{(i)}_{1m,k}\mathrm{e}^{-dz} + \right.\right.$$
$$\left.\left.B^{(i)}_{2m,k}\mathrm{e}^{dz}) + 2pj\{(T^{(i)}_{1m,k} - R^{(i)}_{1m,k})\mathrm{e}^{-jz} + (T^{(i)}_{2m,k} + R^{(i)}_{2m,k})\mathrm{e}^{jz}\}\right]pJ_{m-1}(pr)\mathrm{d}p\right\}\cos\left[m\theta - \frac{k-1}{2}\pi\right], \tag{33}$$

$$u^{(i)}_z(r,\theta,z) = \sum_{m=0}^{\infty}\sum_{k=1}^{2}\left\{\int_0^{\infty}\left[-c(A^{(i)}_{1m,k}\mathrm{e}^{-cz} - A^{(i)}_{2m,k}\mathrm{e}^{cz}) - d(B^{(i)}_{1m,k}\mathrm{e}^{-dz} - B^{(i)}_{2m,k}\mathrm{e}^{dz})\right.\right.$$
$$\left.\left.+p^2(R^{(i)}_{1m,k}\mathrm{e}^{-jz} + R^{(i)}_{2m,k}\mathrm{e}^{jz})\right]pJ_m(pr)\mathrm{d}p\right\}\cos\left[m\theta + \frac{k-1}{2}\pi\right]. \tag{34}$$

At the ground surface $z = 0$, the displacement components are reduced to

$$u_r(r,\theta,0) = \frac{1}{2}\sum_{m=0}^{\infty}\int_0^{\infty} p\Big\{\frac{G}{f}[2p^3a_2j\mathrm{e}^{-cz'} - 2p^3a_1j\mathrm{e}^{-dz'} + pj(a_1-a_2)(2p^2-s^2)\mathrm{e}^{-jz'}](\tilde{f}_{(r-\theta)m,1}\cos m\theta$$
$$-\tilde{f}_{(r-\theta)m,2}\sin m\theta)[J_{m+1}(pr) - J_{m-1}(pr)] + \frac{1}{f}[2a_2pcj\mathrm{e}^{-cz'} - 2pa_1dj\mathrm{e}^{-dz'} + p(a_1-a_2)$$
$$\times(2p^2-s^2)\mathrm{e}^{-jz'}](\tilde{f}^m_{zm,1}\cos m\theta - \tilde{f}^m_{zm,2}\sin m\theta)[J_{m+1}(pr) - J_{m-1}(pr)] + \frac{p}{2j}\mathrm{e}^{-jz'}$$
$$\times(\tilde{f}_{(r+\theta)m,1}\cos m\theta - \tilde{f}_{(r+\theta)m,2}\sin m\theta)[J_{m+1}(pr) + J_{m-1}(pr)]\Big\}\mathrm{d}p, \tag{35}$$

$$u_\theta(r,\theta,0) = \frac{1}{2}\sum_{m=0}^{\infty}\int_0^{\infty} p\Big\{\frac{G}{f}[2p^3a_2j\mathrm{e}^{-cz'} - 2p^3a_1j\mathrm{e}^{-dz'} + pj(a_1-a_2)(2p^2-s^2)\mathrm{e}^{-jz'}](\tilde{f}_{(r-\theta)m,1}\sin m\theta$$
$$+\tilde{f}_{(r-\theta)m,2}\cos m\theta)[J_{m+1}(pr) + J_{m-1}(pr)] + \frac{1}{f}[2a_2pcj\mathrm{e}^{-cz'} - 2pa_1dj\mathrm{e}^{-dz'} + p(a_1-a_2)$$
$$\times(2p^2-s^2)\mathrm{e}^{-jz'}](\tilde{f}^m_{zm,1}\sin m\theta + \tilde{f}^m_{zm,2}\cos m\theta)[J_{m+1}(pr) + J_{m-1}(pr)] + \frac{p}{2j}\mathrm{e}^{-jz'}$$
$$\times(\tilde{f}_{(r+\theta)m,1}\sin m\theta + \tilde{f}_{(r+\theta)m,2}\cos m\theta)[J_{m+1}(pr) - J_{m-1}(pr)]\Big\}\mathrm{d}p, \tag{36}$$

$$u_z(r,\theta,0) = \sum_{m=0}^{\infty}\int_0^{\infty} p\Big\{\frac{G}{f}[-(2p^2-s^2)a_2p^2\mathrm{e}^{-cz'} + (2p^2-s^2)a_1p^2\mathrm{e}^{-dz'} - 2p^2j(da_1-ca_2)$$
$$\times\mathrm{e}^{-jz'}](\tilde{f}_{(r-\theta)m,1}\cos m\theta - \tilde{f}_{(r-\theta)m,2}\sin m\theta) + \frac{1}{f}[-a_2c(2p^2-s^2)\mathrm{e}^{-cz'} + a_1d(2p^2-s^2)\mathrm{e}^{-dz'}$$
$$-2(a_1d-a_2c)p^2\mathrm{e}^{-jz'}](\tilde{f}^m_{zm,1}\cos m\theta - \tilde{f}^m_{zm,2}\sin m\theta)\Big\}J_m(pr)\mathrm{d}p. \tag{37}$$

The solutions for the displacements given by Eqs. (32)–(37) involve the integral of a rapidly oscillatory function over a semi-infinite interval. Due to the complexity of the integrands, these integrals will be evaluated numerically. It is important to note that f occurring in denominators of the integrands has complex roots as a result of considering the dissipative nature of the soil, i.e., the internal friction due to the relative motion between the solid matrix and the pore water. Thus, no singularities are encountered in the real axis p and the numerical integration can be directly performed along this axis. We further remark that the semi-infinite integrals for the inverse Hankel transforms are truncated at some large values and numerically evaluated using *Mathematica* [31]. It is found that such a treatment generally gives satisfactory results.

5. Comparison with existing solutions for purely elastic soil

Solution of the classical Lamb's problem involving an elastic half space subjected to a uniform horizontal buried loading of radius a at $z = z'$ with resultant load of unit is considered in this section. The objective is to verify the foregoing solutions for the purely elastic case and compare the corresponding numerical results with those in [5].

The dynamic response of an elastic half space can be treated as a limiting case of a dry soil in the absence of pore water. This can be accomplished by taking $\rho_w = b = \vartheta = 0$. It then follows that $\beta_1 = \rho\omega^2/(\lambda+2G)$, $\beta_2 = 0$, $p_1 = \sqrt{\rho\omega^2/(\lambda+2G)}$, $(\mathrm{Re}[p_1] \geqslant 0)$, $P_2 = 0$, $s = \sqrt{\rho\omega^2/G}$, $(\mathrm{Re}[s] \geqslant 0)$, $c = \sqrt{p^2 - \rho\omega^2/(\lambda+2G)}$, $d = p$, $j = \sqrt{p^2 - \rho\omega^2/G}$, $a_1 = 0$, and $f = -a_2[G(p^2+j^2)^2 - 4p^2jGc]$, in which p_1 and s are the wave numbers of the corresponding elastic P and S waves, respectively.

Furthermore, for the horizontal load patch case, the loading coefficients defined in Eq. (29) can be expressed by the relations

$$\tilde{f}_{(r-\theta)m,k}(r,z') = \begin{cases} -\frac{J_1(pa)}{\pi Gap^2}, & m=1,\ k=1 \\ 0, & \text{all else cases} \end{cases}, \tag{38a}$$

$$\tilde{f}_{(r+\theta)m,k}(r,z') = \begin{cases} \frac{2J_1(pa)}{\pi Gap^2}, & m=1,\ k=1 \\ 0, & \text{all else cases} \end{cases}, \tag{38b}$$

$$\tilde{f}_{zm,k}(r,z')=0, \quad k=1,2; \quad m=0,1,2,\ldots. \tag{38c}$$

Substitution of Eq. (38) into Eqs. (35)–(37) reduces the displacement components at the ground surface to

$$u_z=\frac{\cos\theta}{2\pi Ga}\int_0^\infty \frac{J_1(pa)[-p(2p^2-s^2)\mathrm{e}^{-cz'}+2pjc\mathrm{e}^{-jz'}]}{[(p^2+j^2)^2-4p^2jc]}[J_2(pr)+J_0(pr)]\mathrm{d}p, \tag{39a}$$

$$u_r=\frac{\cos\theta}{2\pi Ga}\int_0^\infty \frac{J_1(pa)[2p^2j\mathrm{e}^{-cz'}-j(2p^2-s^2)\mathrm{e}^{-jz'}]}{[(p^2+j^2)^2-4p^2jc]}[J_2(pr)-J_0(pr)]\mathrm{d}p + \frac{\cos\theta}{2\pi Ga}\int_0^\infty \frac{J_1(pa)\mathrm{e}^{-jz'}}{j}[J_2(pr)+J_0(pr)]\mathrm{d}p, \tag{39b}$$

$$u_\theta=\frac{\sin\theta}{2\pi Ga}\int_0^\infty \frac{J_1(pa)[2p^2j\mathrm{e}^{-cz'}-j(2p^2-s^2)\mathrm{e}^{-jz'}]}{[(p^2+j^2)^2-4p^2jc]}[J_2(pr)+J_0(pr)]\mathrm{d}p + \frac{\sin\theta}{2\pi Ga}\int_0^\infty \frac{J_1(pa)\mathrm{e}^{-jz'}}{j}[J_2(pr)-J_0(pr)]\mathrm{d}p. \tag{39c}$$

This result, after appropriate manipulation, is exactly the same expression for the surface displacements of an elastic half space derived by Pak [5]. It should, however, be mentioned that in the elastic case, the denominator of the integrand in the integrals given by Eq. (39) has poles along the real axis. Hence, the path of integration needs to be deformed around the respective singularities.

Alternatively, the case of a dry soil subjected to horizontal patch load of radius a and unit intensity can be numerically solved from Eqs. (32)–(34), provided that the corresponding parameters of a saturated soil are selected to approach an elastic case. For convenience, in the numerical study, the radius a is selected to normalize all length parameters including the coordinate frame and the mass density of bulk material ρ to normalize all mass-like parameters, while the stresses and

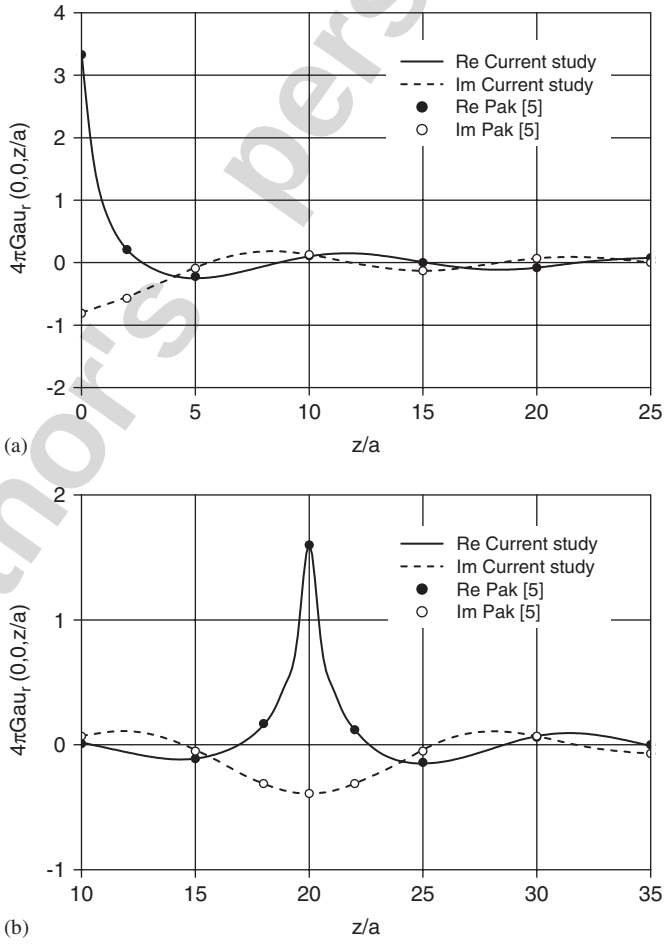

Fig. 2. Radial displacement u_r under unit buried horizontal load on a circular region. (a) $z'/a=0$ and (b) $z'/a=20$.

pore pressure are normalized with respect to the shear modulus of the solid skeleton. To check our solutions for the reduced purely elastic case, we let the dimensionless parameters be $\bar{M} = M/G = 0.01$, $\bar{\vartheta} = \vartheta/\rho = 0.01$, $\alpha = 0.01$, $\bar{b} = ab/\sqrt{\rho G} = 0.01$, $\bar{\rho}_w = \rho_w/\rho = 0.01$, $a_0 = \sqrt{\rho/G}\,\omega a = 0.5$. Fig. 2 presents the normalized horizontal displacement in the x-direction along the z-axis (i.e., $r = \theta = 0$) for a surface source $\bar{z}' = z'/a = 0$ (Fig. 2(a)) and a buried source $\bar{z}' = z'/a = 20$ (Fig. 2(b)), which is compared with the numerical result by Pak [5]. As can be seen from Fig. 2, the two solutions are in excellent agreement.

6. Numerical results for saturated soils

In this section, numerical results for the dynamic response of a semi-infinite saturated soil due to buried sources are presented. For illustrative purpose, a uniformly distributed horizontal load of radius a with unit resultant (i.e., $\pi a^2 q = 1$, where q is the horizontal load density) was considered. The following dimensionless material parameters were adopted in the numerical analysis: $\bar{\lambda} = \lambda/G = 1.5$, $\bar{M} = M/G = 12.2$, $\bar{\vartheta} = \vartheta/\rho = 1.1$, $\alpha = 0.97$, $\bar{b} = ab/\sqrt{\rho G} = 2.3$, $\bar{\rho}_w = \rho_w/\rho = 0.53$, with the depth of the source $\bar{z}' = z'/a$ ranging from 1 to 10. The dimensionless exciting frequency is again assumed to be $a_0 = 0.5$.

Combining Eqs. (32)–(34) and (38), the displacements u_r, u_θ and u_z of the soil frame due to the buried horizontal load can be evaluated. Since both the vertical and angular displacements along the z-axis are equal to zero, only the radial displacement u_r responses for the applied loading located at depth $z'/a = 1$, 2, 5 and 10 are depicted (Fig. 3). The results are presented in terms of the normalized radial displacement in the r direction $4\pi G a u_r(0, 0, z/a)$ against the depth z/a, and presented in complex notation, with the real and imaginary parts corresponding to the in-phase and the 90° out-of-phase components, respectively. It is found that the general trend in the variation of the radial displacements with depth is quite similar for different loading levels. In all cases, the responses show distinct oscillations with decreasing magnitudes for increasing field depth z/a. As for the case of the ideal elastic half space, the real parts of the displacements exhibit sharp peaks which correspond exactly to the loading levels (Fig. 3(a)), whilst the imaginary parts vary smoothly at these levels. This is reasonable since the real part represents the response of the saturated soil at the instant the load reaches its maximum value, whilst the imaginary part corresponds to the response of the saturated soil at the instant of vanishing loading [5].

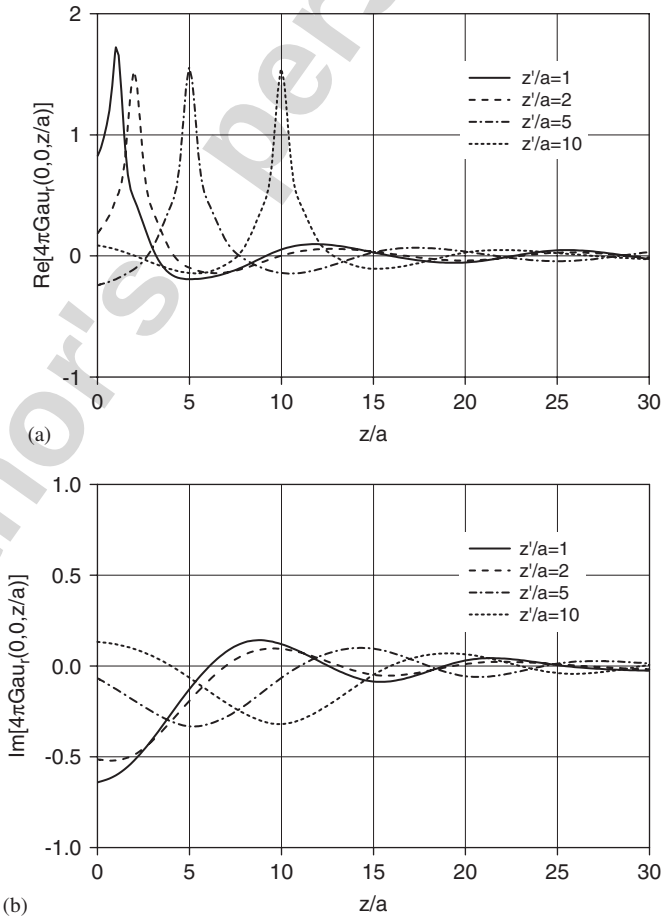

Fig. 3. Radial displacement u_r under unit buried horizontal load on a circular region. (a) Real part and (b) imaginary part.

To investigate the influence of pore water on the dynamic soil response, Fig. 4 presents the comparison of the radial displacement u_r between the saturated soil and the corresponding ideal elastic case. Note that the parameters used in the numerical calculation are the same as those in Fig. 3, except that the nondimensional frequency for the elastic case has been modified to be $a_0' = \sqrt{1-(\bar{\rho}_w^2/\bar{m})}\, a_0$ for the sake of comparison [32]. It is interesting to find that the effect of pore water is negligible. This is not surprising because for a small value of $\bar{b} = 2.3$, the pore pressure dissipates quickly and the saturated soil will thus behave closely to the reduced elastic case.

Figs. 5 and 6 show, respectively, the variation of the amplitude of the normalized radial and vertical displacements along the surface ($\theta = z = 0$). The amplitude of the circumferential displacement along the surface is in fact identical to zero

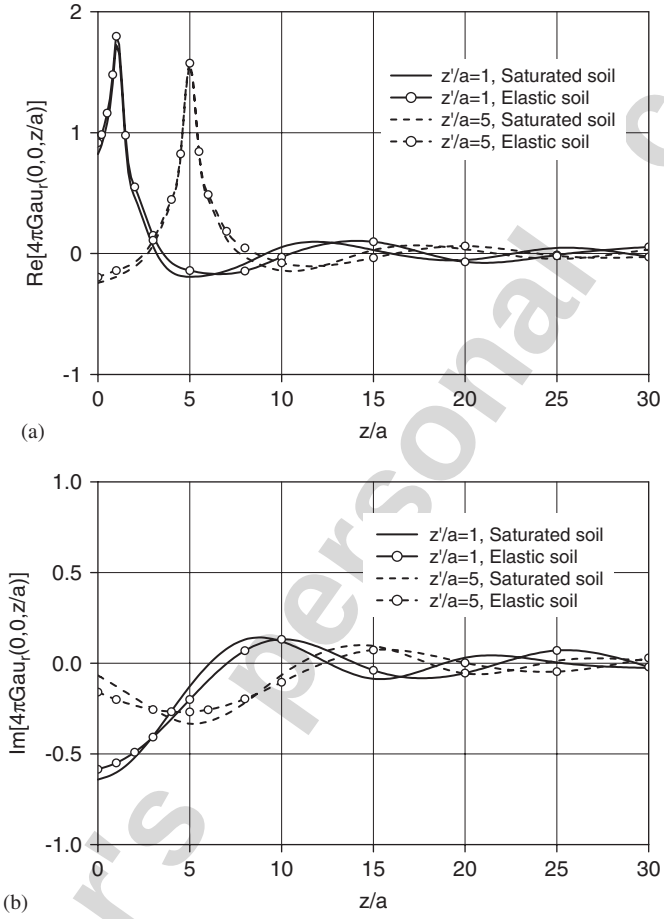

Fig. 4. Comparison of radial displacement u_r between saturated soil and ideal elastic case. (a) Real part and (b) imaginary part.

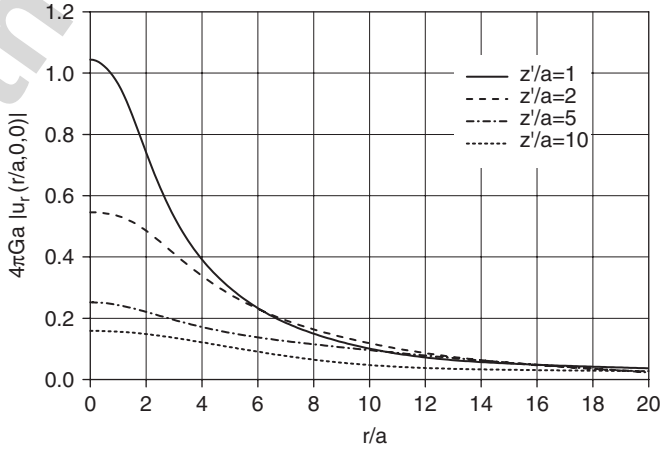

Fig. 5. Amplitudes of nondimensional surface radial displacements with $\theta = 0$.

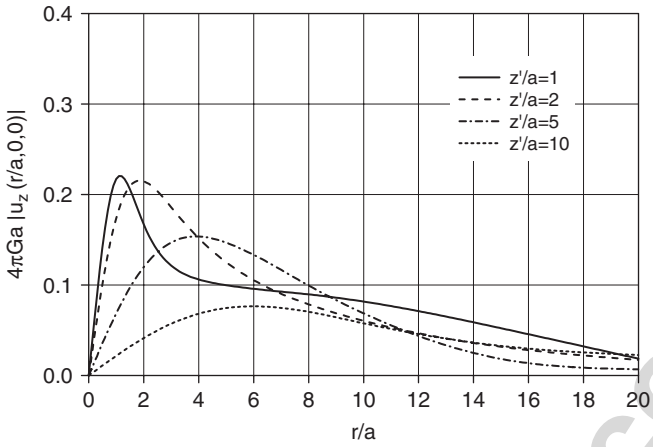

Fig. 6. Amplitudes of nondimensional surface vertical displacements with $\theta = 0$.

because of symmetry. It is observed from Figs. 5 and 6 that the amplitude of the vertical displacement is much smaller than that of the corresponding radial displacement, in particular near the z-axis. This feature is consistent with the nature of the horizontal buried loading. Moreover, at the fixed surface location r close to the z-axis, the amplitude of u_r decreases rapidly with increasing loading depth whilst the influence of the loading level on u_z is less pronounced. It is also noted that the amplitude of the radial displacement decreases monotonously with increasing distance r. However, oscillatory variation behavior is observed for the surface vertical displacements. Generally, the amplitude of u_z increases with r until a maximum value is reached at certain horizontal distance; after that it then decreases monotonously to zero. The peak location of the vertical displacement advances in r with increasing loading depth z'/a.

7. Conclusions

A semi-analytical solution for the 3D Green function of a poroelastic half space subjected to an arbitrary buried loading is presented in this paper. The mathematical approach is based on integral transform techniques. Solutions for the skeleton displacements, stresses, and pore pressure are derived in terms of integral representations. It is shown that, in the absence of saturating pore fluid, our results reduce to the well-known solutions of the Lamb's problem for the purely elastic half space.

The dynamic response of a semi-infinite saturated soil due to a uniform circular horizontal loading located at different depths below the surface are also computed numerically. It is found that the general trends of variations of the radial displacements along the z-axis are quite similar for different loading levels. The real parts of the displacements increase sharply at the corresponding loading levels, whilst the imaginary parts vary smoothly at these levels. For highly permeable soils, presence of pore water has negligible influence on the displacement response. The numerical results also show that the amplitudes of the vertical displacements along the surface are smaller than that of the corresponding radial displacements, and are less influenced by the loading levels as compared to the radial components. In addition, the radial displacements decrease rapidly with increasing loading depth whilst the surface vertical displacements show oscillatory variations. The buried loading Green's functions developed in this paper can be used to solve a variety of 3D boundary-value problems of dynamic poroelasticity.

References

[1] Lamb H. On the propagation of tremors on the surface of an elastic solid. Philos Trans R Soc London Ser A 1904;203:1–42.
[2] Newlands M. Lamb's problems with internal dissipation. J Acoust Soc Am 1954;26:434–49.
[3] Perkeris CL. The seismic surface pulse. Proc Nat Acad Sci 1955;41:469–80.
[4] Perkeris CL. The seismic buried pulse. Proc Nat Acad Sci 1955;41:629–39.
[5] Pak RYS. Asymmetric wave propagation in an elastic half-space by a method of potentials. J Appl Mech 1987;54:121–6.
[6] Rajapakse RKND, Wang Y. Elastodynamic Green's functions of orthotropic half space. J Eng Mech ASCE 1991;117:588–604.
[7] Rajapakse RKND, Wang Y. Green's functions for transversely isotropic elastic half space. J Eng Mech ASCE 1993;119:1724–46.
[8] Wang CY, Achenbach JD. Lamb's problem for solids of general anisotropy. Wave Motion 1996;24:227–42.
[9] Biot MA. The theory of propagation of elastic waves in a fluid-saturated porous solid. I, low frequency range. J Acoust Soc Am 1956;28:168–78.
[10] Biot MA. The theory of propagation of elastic waves in a fluid-saturated porous solid. II, high frequency range. J Acoust Soc Am 1956;28:179–91.
[11] Biot MA. General theory of three-dimensional consolidation. J Appl Phys 1941;12:155–64.
[12] Biot MA. Theory of elasticity and consolidation for a porous anisotropic solid. J Appl Phys 1955;26:182–5.
[13] Biot MA. Mechanics of deformation and acoustic propagation in porous media. J Appl Phys 1962;33:1482–98.

[14] Selvadurai APS. Mechanics of poroelastic media. Boston, MA, USA: Kluwer Academic Publishers; 1996.
[15] Cheng AHD, Detournay E, Abousleiman Y, Rajapakse RKND. Poroelasticity. Maurice A. Biot memorial issue. Int J Solids Struct 1998;35.
[16] Pan E. Green's functions in layered poroelastic half-spaces. Int J Num Analy Methods Geomech 1999;23:1631–53.
[17] Theodorakopoulos DD, Chassiakos AP, Beskos DE. Dynamic effects of moving load on a poroelastic soil medium by an approximate method. Int J Solids Struct 2004;41:1801–22.
[18] Manolis GD, Beskos DE. Integral formulation and fundamental solution of dynamic poroelasticity and thermoelasticity. Acta Mech 1989;76:89–104.
[19] Manolis GD, Beskos DE. Errata in 'Integral formulation and fundamental solution of dynamic poroelasticity and thermoelasticity'. Acta Mech 1990;83:223–6.
[20] Simon B, Zienkiewicz OC, Paul D. An analytical solution for the transient response of saturated porous elastic solids. Int J Num Analy Methods Geomech 1984;8:381–98.
[21] Paul S. On the displacement produced in a porous elastic half-space by an impulsive line load (non-dissipative case). Pure Appl Geophys 1976;114:605–14.
[22] Paul S. On the disturbance produced in a semi-infinite poroelastic medium by a surface load. Pure Appl Geophys 1976;114:615–27.
[23] Halpern MR, Christiano P. Response of poroelastic halfspace to steady-state harmonic surface tractions. Int J Num Analy Methods Geomech 1986;10:609–32.
[24] Philippacopoulos AJ. Lamb's problem for fluid-saturated, porous media. Bull Seism Soc Am 1988;78:908–23.
[25] Senjuntichai T, Rajapakse RKND. Dynamic Green's functions of homogeneous poroelastic half-space. J Eng Mech ASCE 1994;120:2381–404.
[26] Sejuntichai T, Sapsathiarn Y. Forced vertical vibration of circular plate in multilayered poroelastic medium. J Eng Mech ASCE 2003;129:1330–41.
[27] Philippacopoulos AJ. Buried point source in a poroelastic half-space. J Eng Mech ASCE 1997;123:860–9.
[28] Jin B, Liu H. Dynamic response of a poroelastic half space to horizontal buried loading. Int J Solids Struct 2001;38:8053–64.
[29] Zhou XL, Wang JH, Lu JF. Transient foundation solution of saturated soil to impulsive concentrated loading. Soil Dyn Earthquake Eng 2002;22:273–81.
[30] Muki R. Asymmetric problem of the theory of elasticity for a semi-infinite solid and a thick plate. Sneddon IN, Hill R, editors. Progress in Solid Mechanics (I). Amsterdam: North Holland; New York: Interscience; 1960. p. 399.
[31] Wolfram S. Mathematica: a system for doing mathematics by computer. Reading, MA: Addison-Wesley; 1988.
[32] Chen SL, Chen LZ, Pan E. Vertical vibration of a flexible plate with rigid core on saturated ground. J Eng Mech ASCE 2007;133(3).